

18th December 2019

# The $g - 2$ of charged leptons, $\alpha(M_Z^2)$ and the hyperfine splitting of muonium

Alexander Keshavarzi<sup>1,2</sup>, Daisuke Nomura<sup>3</sup> and Thomas Teubner<sup>4</sup><sup>1</sup>*Department of Physics and Astronomy, The University of Manchester, Manchester M13 9PL, United Kingdom*<sup>2</sup>*Department of Physics and Astronomy, The University of Mississippi, Mississippi 38677, U.S.  
Email: alexander.keshavarzi@manchester.ac.uk*<sup>3</sup>*KEK Theory Center, Tsukuba, Ibaraki 305-0801, Japan  
Email: dnomura@post.kek.jp*<sup>4</sup>*Department of Mathematical Sciences, University of Liverpool, Liverpool L69 3BX, United Kingdom  
Email: thomas.teubner@liverpool.ac.uk*

## Abstract

Following updates in the compilation of  $e^+e^- \rightarrow$  hadrons data, this work presents re-evaluations of the hadronic vacuum polarisation contributions to the anomalous magnetic moment of the electron ( $a_e$ ), muon ( $a_\mu$ ) and tau lepton ( $a_\tau$ ), to the ground-state hyperfine splitting of muonium and also updates the hadronic contributions to the running of the QED coupling at the mass scale of the  $Z$  boson,  $\alpha(M_Z^2)$ . Combining the results for the hadronic vacuum polarisation contributions with recent updates for the hadronic light-by-light corrections, the electromagnetic and the weak contributions, the deviation between the measured value of  $a_\mu$  and its Standard Model prediction amounts to  $\Delta a_\mu = (28.02 \pm 7.37) \times 10^{-10}$ , corresponding to a muon  $g - 2$  discrepancy of  $3.8\sigma$ .

# Contents

<b>1</b>	<b>Introduction</b>	<b>2</b>
<b>2</b>	<b>Updates since the last analysis (KNT18)</b>	<b>4</b>
2.1	$\pi^+\pi^-$ channel . . . . .	4
2.2	$\pi^+\pi^-\pi^0$ channel . . . . .	6
2.3	Other channels . . . . .	8
<b>3</b>	<b>Results</b>	<b>9</b>
3.1	The anomalous magnetic moment of the electron, $a_e$ . . . . .	9
3.2	The anomalous magnetic moment of the muon, $a_\mu$ . . . . .	12
3.3	The anomalous magnetic moment of the tau lepton, $a_\tau$ . . . . .	16
3.4	Determination of $\alpha(M_Z^2)$ . . . . .	17
3.5	The hyperfine splitting of muonium, $\Delta\nu_{\text{Mu}}^{\text{had,VP}}$ . . . . .	18
<b>4</b>	<b>Conclusions and future prospects</b>	<b>20</b>

## 1 Introduction

For the charged leptons ( $l = e, \mu, \tau$ ), the study of their anomalous magnetic moment,  $a_l = (g - 2)_l/2$ , continues to serve as a long-standing test of the Standard Model (SM) and as a powerful indirect search of new physics. In each case, the SM prediction of the anomalous magnetic moment is determined by summing the contributions from all sectors of the SM, such that

$$a_l^{\text{SM}} = a_l^{\text{QED}} + a_l^{\text{EW}} + a_l^{\text{had,VP}} + a_l^{\text{had,LbL}}, \quad (1.1)$$

where  $a_l^{\text{QED}}$  are the QED contributions,  $a_l^{\text{EW}}$  are the (electro-)weak (EW) contributions,  $a_l^{\text{had,VP}}$  are the hadronic (had) vacuum polarisation (VP) contributions and  $a_l^{\text{had,LbL}}$  are those contributions due to hadronic light-by-light (LbL) scattering.

The recent complete re-evaluation of the hadronic VP contributions to  $a_\mu$  preceding this work (denoted as KNT18) found the SM prediction to be  $a_\mu^{\text{SM}}(\text{KNT18}) = (11\,659\,182.04 \pm 3.56) \times 10^{-10}$  [1], with the uncertainty still entirely dominated by the non-perturbative, hadronic sector. Compared with the current experimental world average of  $a_\mu^{\text{exp}} = (11\,659\,209.1 \pm 6.3) \times 10^{-10}$  [2–5], a discrepancy of  $\Delta a_\mu = a_\mu^{\text{exp}} - a_\mu^{\text{SM}} = (27.06 \pm 7.26) \times 10^{-10}$  was found, with the SM prediction being  $3.7\sigma$  below the experimental measurement. With new efforts at Fermilab (FNAL) [6, 7] (and later at J-PARC [8]) aiming to reduce the experimental uncertainty by a factor of four, coupled with the ongoing efforts of the Muon  $g - 2$  Theory Initiative [9] to improve the determination of the various SM contributions in conjunction with these new measurements, it is imperative that the determination in [1] is continuously updated and improved.

A relatively new and interesting deviation has now also arisen in the study of the electron  $g - 2$ . Until recently, the comparison of the exceptionally precise measurement of  $a_e^{\text{exp}} = (1\,159\,652\,180.73 \pm 0.28) \times 10^{-12}$  [10] with the SM prediction  $a_e^{\text{SM}}(\alpha_{\text{Rb}}) = (1\,159\,652\,182.032 \pm 0.720) \times 10^{-12}$  [11] (which updated [12]) deviated only at the level of  $1.7\sigma$ . Here,  $\alpha_{\text{Rb}}$  denotes that the SM prediction has been determined using the measurement of the fine-structure constant via rubidium (Rb) atomic interferometry [13], which contributes the dominant uncertainty to this prediction of  $a_e^{\text{SM}}$ . However, the use of a new, more precise measurement of  $\alpha$  using caesium (Cs)

atomic interferometry [14] results in an estimate of  $a_e^{\text{SM}}(\alpha_{\text{Cs}}) = (1\,159\,652\,181.61 \pm 0.23) \times 10^{-12}$ . This implies a deviation of  $\Delta a_e = a_e^{\text{exp}} - a_e^{\text{SM}}(\alpha_{\text{Cs}}) = (-0.88 \pm 0.36) \times 10^{-12}$ , corresponding to a  $2.5\sigma$  difference.<sup>1</sup> This result has invoked much theoretical work into the possibility of simultaneously explaining the differences in both the electron and muon sector, which must also explain the current sign difference seen between  $\Delta a_e$  and  $\Delta a_\mu$  (see e.g. [16]). Although, due to the small mass of the electron,  $a_e^{\text{SM}}$  is less sensitive to strong effects than  $a_\mu^{\text{SM}}$ , the recently observed changes in the electron sector make it important that the hadronic contributions to the electron  $g - 2$  are also updated from the previous determination in [17] (denoted here as NT12).

Measurements of the anomalous magnetic moment of the tau lepton,  $a_\tau^{\text{exp}}$ , are notoriously difficult due to the short lifetime of the  $\tau$  and, as such, no direct measurement of  $a_\tau$  has yet been achieved. Limits on  $a_\tau^{\text{exp}}$  were set by the DELPHI collaboration to be  $-0.052 < a_\tau^{\text{exp}} < 0.013$  at the 95% confidence level [2, 18], which is quoted in the form  $a_\tau^{\text{exp}} = -0.018(17)$  in [18]. By standard lepton mass-scaling arguments,  $a_\tau$  is more sensitive to heavy new physics than  $a_\mu$  by a factor of  $m_\tau^2/m_\mu^2 \sim 280$ . However, the relative contributions of strong effects compared to both the electron and the muon make  $a_\tau$  more sensitive to hadronic contributions by the same argument. The hadronic VP contributions were determined in [19] to be  $a_\tau^{\text{had, VP}} = (345.1 \pm 3.9) \times 10^{-8}$ , resulting (along with calculations of the various other SM contributions) in  $a_\tau^{\text{SM}} = (117\,721 \pm 5) \times 10^{-8}$ . Although it is clear that the comparison of  $\Delta a_\tau = a_\tau^{\text{exp}} - a_\tau^{\text{SM}}$  is insignificant due to the current insufficient accuracy of  $a_\tau^{\text{exp}}$ , the determination of  $a_\tau^{\text{SM}}$  is an interesting undertaking and may prove useful, should experimental techniques improve to be able to better probe the anomaly of the  $\tau$  lepton.

It follows that this work, denoted KNT19, will update the hadronic vacuum polarisation contributions to  $a_l = (g - 2)_l/2$  for all  $l = e, \mu, \tau$ . These are calculated utilising dispersion integrals and the experimentally measured cross section,

$$\sigma_{\text{had}, \gamma}^0(s) \equiv \sigma^0(e^+e^- \rightarrow \gamma^* \rightarrow \text{hadrons} + \gamma), \quad (1.2)$$

where the superscript 0 denotes the bare cross section (undressed of all vacuum polarisation effects) and the subscript  $\gamma$  indicates the inclusion of effects from final state radiation (FSR) of (one or more) photons (see [1] for details). The determination of the hadronic  $R$ -ratio, defined as

$$R(s) = \frac{\sigma_{\text{had}, \gamma}^0(s)}{\sigma_{\text{pt}}(s)} \equiv \frac{\sigma_{\text{had}, \gamma}^0(s)}{4\pi\alpha^2/(3s)} \quad (1.3)$$

and obtained from the updated compilation of all available  $e^+e^- \rightarrow \text{hadrons}$  data, is the foundation of this endeavour. Here,  $\alpha = \alpha(0)$  is the fine-structure constant. From this, the leading-order (LO) hadronic VP contributions to  $a_l$  can be determined via the dispersion relation

$$a_l^{\text{had, LO VP}} = \frac{\alpha^2}{3\pi^2} \int_{s_{th}}^{\infty} \frac{ds}{s} R(s) K_l(s), \quad (1.4)$$

where  $s_{th} = m_\pi^2$  and  $K_l(s)$  is a well-known kernel function [20, 21]. Expressed in the form  $\hat{K}_l(s) \equiv 3s/m_l^2 K(s)$ ,  $\hat{K}_l(s)$  is a monotonically-increasing function that behaves as  $\hat{K}_l(s) \rightarrow 1$  as  $s \rightarrow \infty$ . This behaviour differs slightly for each lepton. In the case of the electron, the deviation

---

<sup>1</sup>Note that very recently there has been an independent calculation of the purely photonic five-loop contributions to  $a_e$  [15], which gives a different value compared to the one in [11] and which, if adopted, would slightly change the predictions for  $a_e^{\text{SM}}$  and  $\Delta a_e$ .

of  $\hat{K}_e(s)$  from 1 is almost negligible for all  $s$  and causes  $a_e^{\text{had, LO VP}}$  to be heavily dominated by the contributions from the lowest energies [17]. For the muon,  $K_\mu(s)$  behaves as  $K_\mu(s) \sim m_\mu^2/(3s)$  at low energies and also accentuates the low energy domain [1, 22], although not as heavily as for the electron. For  $\hat{K}_\tau(s)$ , the larger  $\tau$  mass results in a functional structure that further increases the role of contributions from higher energies relative to  $\hat{K}_\mu(s)$ , although the role of lower energies is still prominent [19]. At next-to-leading order (NLO), similar dispersion integrals and kernel functions exist [22, 23], allowing for  $a_l^{\text{had, NLO VP}}$  to be determined in conjunction with the LO contributions. At NNLO,  $a_l^{\text{had, NNLO VP}}$  has been determined for  $l = e, \mu$  [24].

In addition, the determination of the hadronic  $R$ -ratio is a crucial input for two other precision observables which test the SM. First, the hadronic contributions to the effective QED coupling  $\Delta\alpha_{\text{had}}^{(5)}(q^2)$  allow for an update of this quantity at the scale of the  $Z$  boson mass,  $\alpha(M_Z^2)$ , which hinders the accuracy of EW precision fits. Second, the hadronic VP corrections are a non-negligible part of the ground-state hyperfine splitting (HFS) of muonium,  $\Delta\nu_{\text{Mu}}$ , which can be used to determine the electron-to-muon mass ratio and, hence, the muon mass.

This paper continues, in Section 2, with a description of the updates in the compilation of hadronic cross data since [1]. Section 3 details the new results for the contributions to  $a_l^{\text{had, LO VP}}$  for each  $l = e, \mu, \tau$  (with corresponding new estimates for  $a_l^{\text{SM}}$ ), followed by updated predictions for  $\alpha(M_Z^2)$  and  $\Delta\nu_{\text{Mu}}^{\text{had, VP}}$ . Conclusions and discussions of future prospects are given in Section 4.

## 2 Updates since the last analysis (KNT18)

The data combination methodology in this work is unchanged from [1] and, unless differences are explicitly stated, the cross section determination for each hadronic channel is unaltered. However, various updates with respect to the available data have been accounted for and are described in the following. As before, results for  $a_\mu^{\text{had, LO VP}}$  are quoted with their respective statistical (stat) uncertainty, systematic (sys) uncertainty, vacuum polarisation (vp) correction uncertainty and final state radiation (fsr) correction uncertainty. The total (tot) uncertainty is determined from the individual sources added in quadrature.

### 2.1 $\pi^+\pi^-$ channel

The all-important  $\pi^+\pi^-$  channel is modified only by the introduction of a new radiative return measurement based on data taken at the CLEO-c experiment between  $0.3 \leq \sqrt{s} \leq 1.0$  GeV, covering the dominant  $\rho$  resonance region [25]. The measurement consists of two data sets: the first taken at  $e^+e^-$  energies at the centre-of-mass of the  $\psi(3770)$  resonance and the second at the  $\psi(4170)$  resonance. Although these measurements come already undressed of VP effects as required by equation (1.2), the undressing procedure applied in [25] used an outdated routine [26]. Therefore, in this work, the published cross section values are redressed utilising the routine provided in [26] and then undressed via the KNT18 vacuum polarisation routine, `vp_knt_v3.0` [1, 27].<sup>2</sup> Notably, the statistical and systematic uncertainties of the CLEO-c data are large compared to the KLOE [28–31] and BaBar [32] measurements and, therefore, cannot resolve the tension between the KLOE and BaBar data. In addition, in the KNT19 data combination, the systematic uncertainties of the two CLEO-c data sets are taken to be 100% correlated, which further limits their influence.

<sup>2</sup>This routine is available for use by contacting the authors directly.

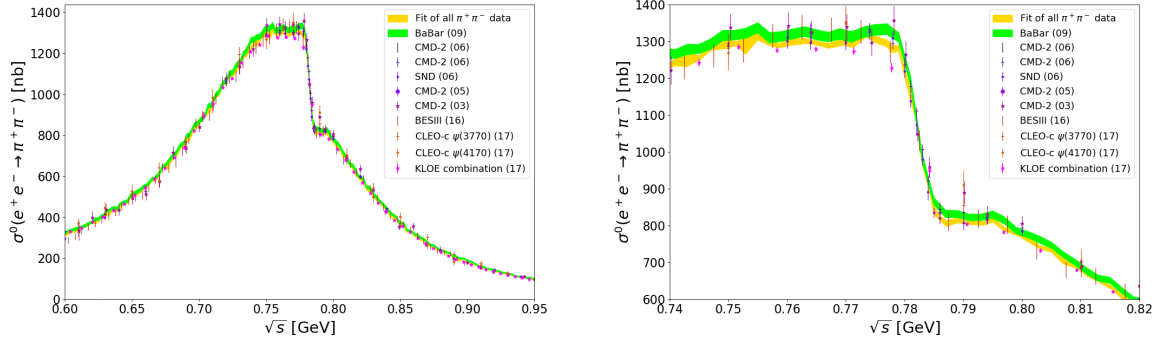


Figure 1: Contributing data in the  $\rho$  resonance region of the  $\pi^+\pi^-$  channel plotted against the new fit of all data (left panel), with an enlargement of the  $\rho$ - $\omega$  interference region (right panel).

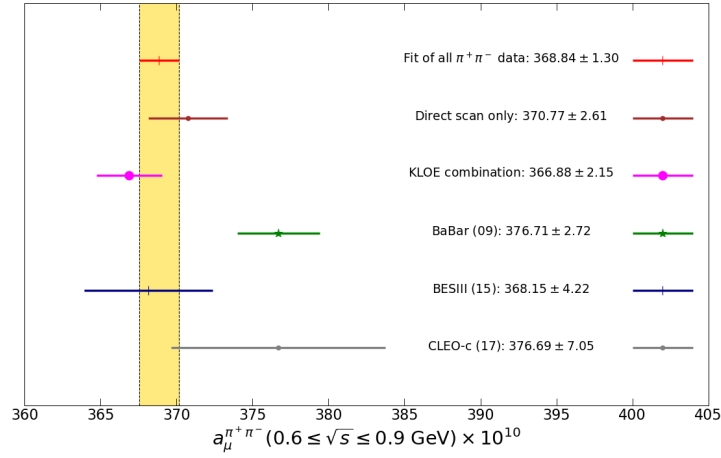


Figure 2: Comparison of the evaluations of  $a_{\mu}^{\pi^+\pi^-}$  from the individual radiative return measurements and the combination of direct scan  $\pi^+\pi^-$  measurements between  $0.6 \leq \sqrt{s} \leq 0.9$  GeV.

The combined cross section and the dominant contributing measurements are displayed in the  $\rho$  region and magnified in the  $\rho$ - $\omega$  interference region in Figure 1. Figure 2 shows the updated comparison of the evaluations of  $a_{\mu}^{\pi^+\pi^-}$  from the radiative return measurements and the combination of remaining direct scan data in the vicinity of the  $\rho$  resonance. Although the new CLEO-c data are compatible with both the KLOE and BaBar measurements, resulting in a marginal improvement in the quality of the overall fit, as expected the combination is largely unchanged due to the large uncertainties of the CLEO-c data. The tension between BaBar and KLOE persists, emanated in the KNT19 combination of all  $\pi^+\pi^-$  data, which is still dominated by the three KLOE cross section measurements and their precise, highly-correlated uncertainties. This is further exemplified by Figure 3, which clearly indicates the tension between KLOE and BaBar, and between the fit of all  $\pi^+\pi^-$  data and BaBar, especially in the high-energy tail of the  $\rho$  resonance.

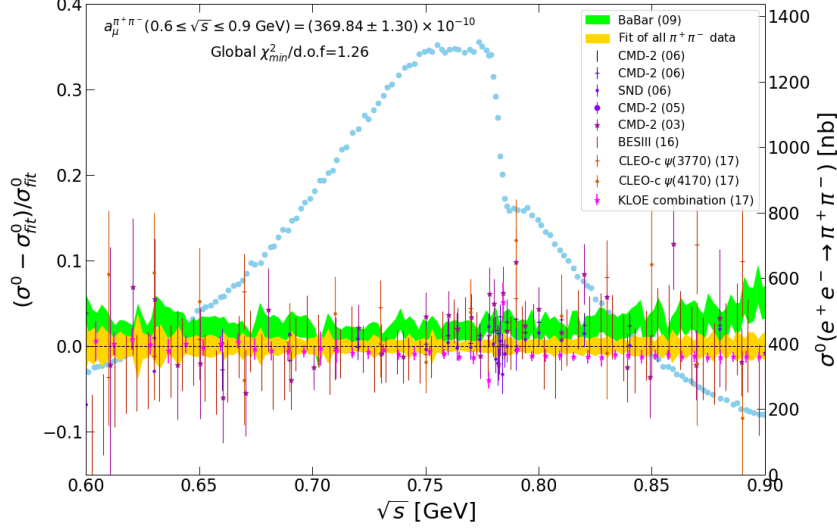


Figure 3: The relative difference of the radiative return and the most relevant of the direct scan data sets contributing to  $a_{\mu}^{\pi^+\pi^-}$ , and the fit of all data. For comparison, the individual sets have been normalised against the fit and have been plotted in the  $\rho$  region. The green band represents the BaBar data and their errors (statistical and systematic, added in quadrature). The yellow band represents the full data combination which incorporates all correlated statistical and systematic uncertainties. However, the width of the yellow band simply displays the square root of the diagonal elements of the total output covariance matrix of the fit.

For the muon  $g - 2$ , the full combination of all  $\pi^+\pi^-$  data gives

$$\begin{aligned} a_{\mu}^{\pi^+\pi^-}[0.305 \leq \sqrt{s} \leq 1.937 \text{ GeV}] &= (503.46 \pm 1.14_{\text{stat}} \pm 1.52_{\text{sys}} \pm 0.06_{\text{vp}} \pm 0.14_{\text{fsr}}) \times 10^{-10} \\ &= (503.46 \pm 1.91_{\text{tot}}) \times 10^{-10}. \end{aligned} \quad (2.1)$$

This value is entirely consistent with [1]. The mean value has increased by  $\sim 25\%$  of the previous error, which itself has reduced by only  $\sim 3\%$ . As before, tensions in the data are accounted for in the local  $\chi^2$  error inflation, increasing the uncertainty of  $a_{\mu}^{\pi^+\pi^-}$  by  $\sim 14\%$ . This has decreased from  $\sim 15\%$  in [1], also reflected in the slight decrease in the global  $\chi^2_{\text{min}}/\text{d.o.f.}(\text{KNT18}) = 1.30$  to  $\chi^2_{\text{min}}/\text{d.o.f.}(\text{KNT19}) = 1.26$  (with 625 d.o.f.).

Although the results of this work are obtained from directly integrating the combined data, detailed analyses employing constraints based on analyticity and unitarity have been performed in [33–37]. These additional constraints have the potential to improve the determination of the two-pion cross section and to possibly reduce the error, especially at low energies where limited data are available. The results obtained in these works are, overall, largely compatible with the determination of this analysis, but lead to slightly larger results for  $a_{\mu}^{\text{had, LO VP}}$  in the energy range  $\sqrt{s} < 0.6 \text{ GeV}$ . A detailed comparison with these values is beyond the scope of this work, but will be presented as part of the studies of the Muon  $g - 2$  Theory Initiative [9].

## 2.2 $\pi^+\pi^-\pi^0$ channel

A recent study of the three-pion contribution to the hadronic vacuum polarisation based on a global fit function using analyticity and unitarity constraints [38] highlighted major differences arising in various determinations of  $a_{\mu}^{\pi^+\pi^-\pi^0}$ . These were attributed to the choice of cross section

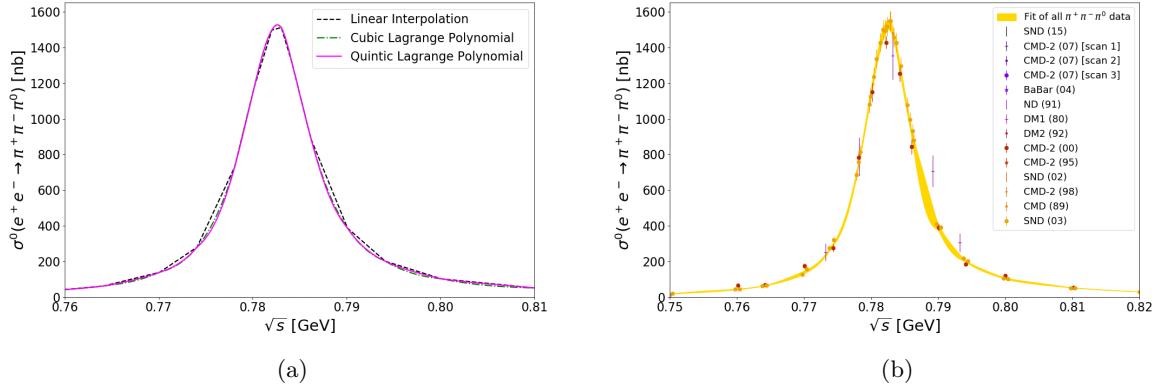


Figure 4: The cross section  $\sigma^0(e^+e^- \rightarrow \pi^+\pi^-\pi^0)$  in the region of the narrow  $\omega$  resonance. In Figure 4(a), the black dashed line, green dashed-dotted line and pink solid line show the linear, cubic and quintic interpolation between clusters, respectively.

interpolation used in the prominent  $\omega$  resonance region when integrating the data. Due to a lack of data and a (relatively) wide-binning in the narrow  $\omega$  resonance itself, the trapezoidal rule integration used in [1, 22, 39, 40], while consistent with the direct data integration procedure utilised in these works, led to a value of  $a_{\mu}^{\pi^+\pi^-\pi^0}$  in [1] larger than found in [37, 38]. In order to address this issue in this work, the clusters and covariance matrix elements corresponding to the fitted  $\omega$  resonance alone have been interpolated to a 0.2 MeV binning using a quintic polynomial. The newly finer-binned resonance, along with the entire  $\pi^+\pi^-\pi^0$  cross section, are then integrated using the trapezoidal rule integral to ensure consistency with the general KNT data combination procedure applied to all other channels. This results in an improved estimate of

$$\begin{aligned} a_{\mu}^{\pi^+\pi^-\pi^0}[0.66 \leq \sqrt{s} \leq 1.937 \text{ GeV}] &= (46.73 \pm 0.32_{\text{stat}} \pm 0.74_{\text{sys}} \pm 0.12_{\text{vp}} \pm 0.47_{\text{fsr}}) \times 10^{-10} \\ &= (46.73 \pm 0.94_{\text{tot}}) \times 10^{-10}, \end{aligned} \quad (2.2)$$

compared to  $a_{\mu}^{\pi^+\pi^-\pi^0}(\text{KNT18}) = (47.79 \pm 0.89) \times 10^{-10}$  in [1]. Figure 4(a) shows an enlargement of the  $\omega$  resonance region, where the comparison between the previously used trapezoidal rule integral (black dashed line), a cubic polynomial interpolation (dashed-dotted green line) and the quintic polynomial (solid pink line) interpolation are visible, highlighting the improvement that this change has made.<sup>3</sup> It can also be seen here that whilst the linear interpolation clearly overestimates the resonance in the tails, the cubic interpolation seemingly underestimates and overestimates the cross section in various places in the tail, hence the choice of the quintic polynomial. The resulting KNT19 determination of the  $\omega$  resonance in the  $\pi^+\pi^-\pi^0$  channel and all contributing data are shown in Figure 4(b).

<sup>3</sup>Should new data be released that better describe the shape of the  $\omega$  resonance in this channel, then the higher-population of data may render this higher-order polynomial interpolation unnecessary and the trapezoidal integral over the available data may be sufficient.

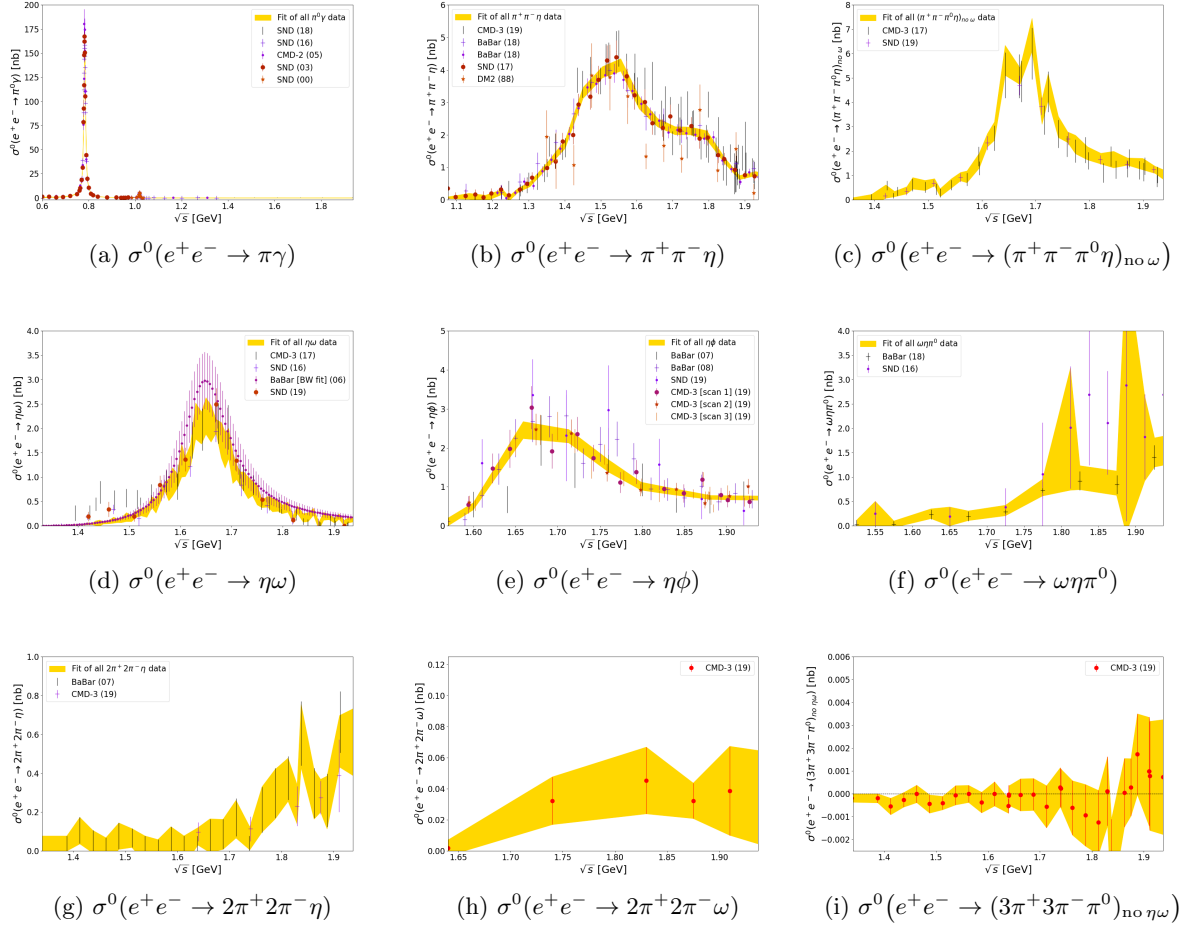


Figure 5: The resulting cross sections of the updated, sub-leading hadronic channels contributing to the KNT19 data compilation.

### 2.3 Other channels

There have been a number of small data updates (see [41–46]) in other channels since [1]. The affected channels are all depicted in Figure 5 and Figure 6. Notably, the  $\pi^0\gamma$  channel now includes a new measurement from the SND experiment [41], which greatly extends the previous upper border of the channel from 1.35 GeV to 1.935 GeV in this work. The changes to  $a_\mu^{\pi^0\gamma}$  are negligible, confirming that no higher energy contributions were missed previously in this hadronic mode.

Two new channels are now included in the KNT19 data compilation. A measurement of the  $2\pi^+2\pi^-\omega$  channel by CMD-3 [46] provides a negligibly small addition to  $a_\mu^{\text{had, LO VP}}$ . This process, together with a measurement of the  $2\pi^+2\pi^-\eta$  mode, have provided the production mechanisms to measure the seven-pion final state  $3\pi^+3\pi^-\pi^0$  in the same work [46], which is the first inclusion of a final state with more than six pions. After removing the contributions from the  $\eta$  and  $\omega$  resonances to avoid double-counting, the  $3\pi^+3\pi^-\pi^0$  channel is statistically consistent with zero below the upper energy boundary of the sum of exclusive states used here, i.e. 1.937 GeV. Once again, it is encouraging to ratify that no large contributions were missed



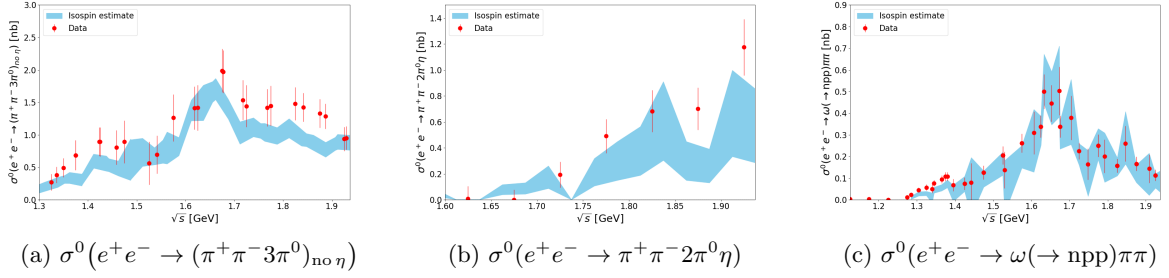


Figure 6: The resulting cross sections of those hadronic channels contributing to the KNT19 data compilation that were previously estimated via isospin relations. In Figure 6(c), the abbreviation ‘ $\rightarrow \text{npp}$ ’ represents the resonant decay to non-purely-pionic modes.

from these channels in the KNT18 data compilation.

Lastly, it is important to mention that the three modes  $\pi^+\pi^-3\pi^0$ ,  $\pi^+\pi^-2\pi^0\eta$  and  $\omega\pi^0\pi^0$  that were previously unmeasured have now been measured by BaBar [42]. These allow, for the first time, for their corresponding hadronic contributions to be estimated using experimental data instead of previously used isospin relations. All three channels are shown in Figure 6, where the agreement in each case between the data and the isospin prediction is good. The resulting integrated contributions to  $a_\mu^{\text{had, LO VP}}$  are all consistent with the theory estimates previously given in [1].

### 3 Results

Table 1 shows the contributions of the individual hadronic channels to  $a_e^{\text{had, LO VP}}$ ,  $a_\mu^{\text{had, LO VP}}$ ,  $a_\tau^{\text{had, LO VP}}$ ,  $\Delta\alpha_{\text{had}}^{(5)}(M_Z^2)$  and  $\Delta\nu_{\text{Mu}}^{\text{had, VP}}$  calculated in this analysis. For  $a_l^{\text{had, LO VP}}$  ( $l = e, \mu, \tau$ ), the combined hadronic cross section data for each channel are integrated according to equation (1.4). To obtain  $\Delta\alpha_{\text{had}}^{(5)}(M_Z^2)$ , the data are integrated using equation (3.14) given in Section 3.4. For  $\Delta\nu_{\text{Mu}}^{\text{had, VP}}$ , equation (3.20) in Section 3.5 is used. In the following section, the KNT19 results for  $a_e$ ,  $a_\mu$ ,  $a_\tau$ ,  $\alpha(M_Z^2)$  and  $\Delta\nu_{\text{Mu}}$  are presented separately. For each of the lepton  $g-2$  results, the values for the LO and NLO hadronic VP contributions as calculated in this work are given, followed by corresponding updated estimates for the respective SM predictions and any necessary discussions.

#### 3.1 The anomalous magnetic moment of the electron, $a_e$

Integrating the updated KNT19 determination of the hadronic  $R$ -ratio described in Section 2 according to equation (1.4) (with  $l = e$ ) results in

$$\begin{aligned}
 a_e^{\text{had, LO VP}} &= (186.08 \pm 0.34_{\text{stat}} \pm 0.53_{\text{sys}} \pm 0.05_{\text{vp}} \pm 0.18_{\text{fsr}}) \times 10^{-14} \\
 &= (186.08 \pm 0.66_{\text{tot}}) \times 10^{-14} .
 \end{aligned}
 \tag{3.1}$$

The contributions from the individual hadronic channels contributing to  $a_e^{\text{had, LO VP}}$  are listed in Table 1. With the same data input, the NLO contributions to  $a_e^{\text{had, VP}}$  are determined here to

Channel	$a_e^{\text{had, LO VP}} \times 10^{14}$	$a_\mu^{\text{had, LO VP}} \times 10^{10}$	$a_\tau^{\text{had, LO VP}} \times 10^8$	$\Delta\alpha_{\text{had}}^{(5)}(M_Z^2) \times 10^4$	$\Delta\nu_{\text{Mu}}^{\text{had, VP}} \text{ (Hz)}$
Chiral perturbation theory (ChPT) threshold contributions					
$\pi^0\gamma$	$0.04 \pm 0.00$	$0.12 \pm 0.01$	$0.03 \pm 0.00$	$0.00 \pm 0.00$	$0.04 \pm 0.00$
$\pi^+\pi^-$	$0.31 \pm 0.01$	$0.87 \pm 0.02$	$0.11 \pm 0.00$	$0.01 \pm 0.00$	$0.25 \pm 0.01$
$\pi^+\pi^-\pi^0$	$0.00 \pm 0.00$	$0.01 \pm 0.00$	$0.00 \pm 0.00$	$0.00 \pm 0.00$	$0.00 \pm 0.00$
$\eta\gamma$	$0.00 \pm 0.00$	$0.00 \pm 0.00$	$0.00 \pm 0.00$	$0.00 \pm 0.00$	$0.00 \pm 0.00$
Exclusive channels ( $\sqrt{s} \leq 1.937 \text{ GeV}$ )					
$\pi^0\gamma$	$1.19 \pm 0.03$	$4.46 \pm 0.10$	$1.75 \pm 0.04$	$0.36 \pm 0.01$	$1.45 \pm 0.03$
$\pi^+\pi^-$	$138.59 \pm 0.54$	$503.46 \pm 1.91$	$172.84 \pm 0.61$	$34.29 \pm 0.12$	$159.64 \pm 0.60$
$\pi^+\pi^-\pi^0$	$12.29 \pm 0.25$	$46.73 \pm 0.94$	$20.47 \pm 0.39$	$4.69 \pm 0.09$	$15.48 \pm 0.31$
$\pi^+\pi^-\pi^+\pi^-$	$3.67 \pm 0.05$	$14.87 \pm 0.20$	$11.50 \pm 0.16$	$4.02 \pm 0.05$	$5.58 \pm 0.08$
$\pi^+\pi^-\pi^0\pi^0$	$4.80 \pm 0.19$	$19.39 \pm 0.78$	$14.56 \pm 0.58$	$5.00 \pm 0.20$	$7.22 \pm 0.29$
$(2\pi^+2\pi^-\pi^0)_{\text{no } \eta\omega}$	$0.24 \pm 0.02$	$0.98 \pm 0.09$	$0.84 \pm 0.08$	$0.32 \pm 0.03$	$0.38 \pm 0.03$
$(\pi^+\pi^-3\pi^0)_{\text{no } \eta}$	$0.15 \pm 0.03$	$0.62 \pm 0.11$	$0.54 \pm 0.10$	$0.21 \pm 0.04$	$0.24 \pm 0.04$
$(3\pi^+3\pi^-)_{\text{no } \omega}$	$0.06 \pm 0.00$	$0.23 \pm 0.01$	$0.21 \pm 0.01$	$0.09 \pm 0.01$	$0.09 \pm 0.01$
$(2\pi^+2\pi^-2\pi^0)_{\text{no } \eta}$	$0.33 \pm 0.04$	$1.35 \pm 0.17$	$1.24 \pm 0.15$	$0.51 \pm 0.06$	$0.53 \pm 0.07$
$(\pi^+\pi^-4\pi^0)_{\text{no } \eta}$	$0.05 \pm 0.05$	$0.21 \pm 0.21$	$0.19 \pm 0.19$	$0.08 \pm 0.08$	$0.08 \pm 0.08$
$(3\pi^+3\pi^-\pi^0)_{\text{no } \eta\omega}$	$0.00 \pm 0.00$	$0.00 \pm 0.01$	$0.00 \pm 0.00$	$0.00 \pm 0.00$	$0.00 \pm 0.00$
$K^+K^-$	$5.86 \pm 0.06$	$23.03 \pm 0.22$	$12.82 \pm 0.12$	$3.37 \pm 0.03$	$8.01 \pm 0.08$
$K_S^0 K_L^0$	$3.33 \pm 0.05$	$13.04 \pm 0.19$	$7.00 \pm 0.10$	$1.77 \pm 0.03$	$4.51 \pm 0.07$
$KK\pi$	$0.66 \pm 0.03$	$2.71 \pm 0.12$	$2.33 \pm 0.10$	$0.89 \pm 0.04$	$1.05 \pm 0.05$
$KK2\pi$	$0.47 \pm 0.02$	$1.93 \pm 0.08$	$1.80 \pm 0.07$	$0.75 \pm 0.03$	$0.76 \pm 0.03$
$KK3\pi$	$0.01 \pm 0.00$	$0.04 \pm 0.02$	$0.04 \pm 0.02$	$0.02 \pm 0.01$	$0.02 \pm 0.01$
$\eta\gamma$	$0.18 \pm 0.01$	$0.70 \pm 0.02$	$0.35 \pm 0.01$	$0.09 \pm 0.00$	$0.24 \pm 0.01$
$\eta\pi^+\pi^-$	$0.33 \pm 0.01$	$1.34 \pm 0.05$	$1.10 \pm 0.04$	$0.41 \pm 0.02$	$0.51 \pm 0.02$
$(\eta\pi^+\pi^-\pi^0)_{\text{no } \omega}$	$0.17 \pm 0.02$	$0.71 \pm 0.08$	$0.63 \pm 0.07$	$0.25 \pm 0.03$	$0.28 \pm 0.03$
$\eta2\pi^+2\pi^-$	$0.02 \pm 0.00$	$0.08 \pm 0.01$	$0.07 \pm 0.01$	$0.03 \pm 0.00$	$0.03 \pm 0.00$
$\eta\pi^+\pi^-\pi^0\pi^0$	$0.03 \pm 0.00$	$0.12 \pm 0.02$	$0.11 \pm 0.02$	$0.05 \pm 0.01$	$0.05 \pm 0.01$
$\eta\omega$	$0.07 \pm 0.01$	$0.30 \pm 0.02$	$0.26 \pm 0.02$	$0.10 \pm 0.01$	$0.11 \pm 0.01$
$\omega(\rightarrow \pi^0\gamma)\pi^0$	$0.22 \pm 0.00$	$0.88 \pm 0.02$	$0.61 \pm 0.01$	$0.19 \pm 0.00$	$0.32 \pm 0.01$
$\omega(\rightarrow \text{npp})2\pi$	$0.03 \pm 0.00$	$0.13 \pm 0.01$	$0.12 \pm 0.01$	$0.04 \pm 0.00$	$0.05 \pm 0.01$
$\omega(\rightarrow \text{npp})3\pi$	$0.04 \pm 0.01$	$0.17 \pm 0.03$	$0.15 \pm 0.03$	$0.06 \pm 0.01$	$0.07 \pm 0.01$
$\omega2\pi^+2\pi^-$	$0.00 \pm 0.00$	$0.01 \pm 0.00$	$0.01 \pm 0.00$	$0.00 \pm 0.00$	$0.00 \pm 0.00$
$\eta\phi$	$0.10 \pm 0.00$	$0.41 \pm 0.02$	$0.37 \pm 0.02$	$0.15 \pm 0.01$	$0.16 \pm 0.01$
$\omega\eta\pi^0$	$0.06 \pm 0.01$	$0.24 \pm 0.05$	$0.23 \pm 0.05$	$0.10 \pm 0.02$	$0.10 \pm 0.02$
$\omega(\rightarrow \text{npp})KK$	$0.00 \pm 0.00$	$0.00 \pm 0.00$	$0.00 \pm 0.00$	$0.00 \pm 0.00$	$0.00 \pm 0.00$
$\eta(\rightarrow \text{npp})KK_{\text{no } \phi \rightarrow KK}$	$0.00 \pm 0.00$	$0.01 \pm 0.01$	$0.01 \pm 0.01$	$0.01 \pm 0.00$	$0.01 \pm 0.01$
$\phi \rightarrow \text{unaccounted}$	$0.01 \pm 0.01$	$0.04 \pm 0.04$	$0.02 \pm 0.02$	$0.01 \pm 0.01$	$0.01 \pm 0.01$
$p\bar{p}$	$0.01 \pm 0.00$	$0.03 \pm 0.00$	$0.03 \pm 0.00$	$0.01 \pm 0.00$	$0.01 \pm 0.00$
$n\bar{n}$	$0.01 \pm 0.00$	$0.03 \pm 0.01$	$0.03 \pm 0.01$	$0.01 \pm 0.00$	$0.01 \pm 0.00$
Other contributions ( $\sqrt{s} > 1.937 \text{ GeV}$ )					
Inclusive channel	$10.38 \pm 0.16$	$43.55 \pm 0.67$	$63.49 \pm 0.91$	$82.78 \pm 1.05$	$19.82 \pm 0.30$
$J/\psi$	$1.49 \pm 0.05$	$6.26 \pm 0.19$	$8.91 \pm 0.27$	$7.07 \pm 0.22$	$2.81 \pm 0.09$
$\psi'$	$0.37 \pm 0.01$	$1.58 \pm 0.04$	$2.50 \pm 0.06$	$2.51 \pm 0.06$	$0.74 \pm 0.02$
$\Upsilon(1S)$	$0.01 \pm 0.00$	$0.05 \pm 0.00$	$0.12 \pm 0.00$	$0.55 \pm 0.02$	$0.03 \pm 0.00$
$\Upsilon(2S)$	$0.00 \pm 0.00$	$0.02 \pm 0.00$	$0.05 \pm 0.00$	$0.24 \pm 0.01$	$0.01 \pm 0.00$
$\Upsilon(3S)$	$0.00 \pm 0.00$	$0.01 \pm 0.00$	$0.03 \pm 0.00$	$0.17 \pm 0.01$	$0.01 \pm 0.00$
$\Upsilon(4S)$	$0.00 \pm 0.00$	$0.01 \pm 0.00$	$0.02 \pm 0.00$	$0.10 \pm 0.01$	$0.00 \pm 0.00$
pQCD ( $\sqrt{s} > 11.199 \text{ GeV}$ )	$0.48 \pm 0.00$	$2.07 \pm 0.00$	$5.33 \pm 0.00$	$124.79 \pm 0.09$	$1.34 \pm 0.00$
Total ( $< \infty \text{ GeV}$ )	$186.08 \pm 0.66$	$692.78 \pm 2.42$	$332.81 \pm 1.39$	$276.09 \pm 1.12$	$232.04 \pm 0.82$

Table 1: Summary of the contributions to  $a_e^{\text{had, LO VP}}$ ,  $a_\mu^{\text{had, LO VP}}$ ,  $a_\tau^{\text{had, LO VP}}$ ,  $\Delta\alpha_{\text{had}}^{(5)}(M_Z^2)$  and  $\Delta\nu_{\text{Mu}}^{\text{had, VP}}$  calculated in this analysis. The first column indicates the channel, the second, third and fourth columns give the contributions to  $a_e^{\text{had, LO VP}}$ ,  $a_\mu^{\text{had, LO VP}}$  and  $a_\tau^{\text{had, LO VP}}$ , whereas the fifth and the last column list the contributions to  $\Delta\alpha_{\text{had}}^{(5)}(M_Z^2)$  and  $\Delta\nu_{\text{Mu}}^{\text{had, VP}}$ , respectively. The last row describes the total contribution obtained from the sum of the individual final states, with the uncertainties added in quadrature.

SM contribution	$a_e(\alpha_{\text{Rb}}) \times 10^{12}$	$a_e(\alpha_{\text{Cs}}) \times 10^{12}$
QED	$1159652180.309 \pm 0.720$ [11]	$1159652179.887 \pm 0.230$ [14]
EW		$0.031 \pm 0.000$ [11]
had LO VP		$1.861 \pm 0.007$
had NLO VP		$-0.223 \pm 0.001$
had NNLO VP		$0.028 \pm 0.000$ [11]
had LbL		$0.037 \pm 0.005$ [11]
Theory total	$1159652182.042 \pm 0.720$	$1159652181.620 \pm 0.230$
Experiment		$1159652180.730 \pm 0.280$ [10]
$\Delta a_e$	$-1.312 \pm 0.773$ (1.7 $\sigma$ )	$-0.890 \pm 0.362$ (2.5 $\sigma$ )

Table 2: Summary of the contributions to  $a_e^{\text{SM}}$ . The values of  $a_e^{\text{QED}}$  from  $\alpha_{\text{Rb}}$  (left) and  $\alpha_{\text{Cs}}$  (right) and their resulting values for  $a_e^{\text{SM}}$  and  $\Delta a_e$  are listed individually for comparison. All results are given as  $a_e^{\text{SM}} \times 10^{12}$ .

be

$$\begin{aligned}
a_e^{\text{had, NLO VP}} &= (-22.28 \pm 0.04_{\text{stat}} \pm 0.06_{\text{sys}} \pm 0.01_{\text{vp}} \pm 0.02_{\text{fsr}}) \times 10^{-14} \\
&= (-22.28 \pm 0.08_{\text{tot}}) \times 10^{-14} .
\end{aligned} \tag{3.2}$$

The NT12 analysis [17] found  $a_e^{\text{had, LO VP}}(\text{NT12}) = (186.6 \pm 1.1) \times 10^{-14}$  and  $a_e^{\text{had, NLO VP}}(\text{NT12}) = (-22.34 \pm 0.14) \times 10^{-14}$ . Comparing the results in this analysis with those from NT12, the mean values have decreased by a substantial fraction of the previously quoted uncertainties (although well within them) and the uncertainties themselves have reduced by  $> 40\%$ . This is in line with the changes noted in the KNT18 determination of  $a_\mu$  [1], which observed similar changes largely due to reductions in the mean value and uncertainty of the dominant  $\pi^+\pi^-$  channel.

As the NNLO hadronic VP contributions are not calculated in this work, the result  $a_e^{\text{had, NNLO VP}} = (2.80 \pm 0.01) \times 10^{-14}$  from [24] is adopted which utilises the HLMNT11 [40] data compilation for the hadronic  $R$ -ratio.<sup>4</sup> For the hadronic LbL contributions, the value  $a_e^{\text{had, LbL}} = (3.7 \pm 0.5) \times 10^{-14}$  from [47] is used. With these, the full hadronic contributions to the electron  $g - 2$  are estimated to be

$$a_e^{\text{had}} = (170.30 \pm 0.77_{\text{tot}}) \times 10^{-14} , \tag{3.3}$$

where, due to the complete correlations from the same input  $R$ -ratio, the errors of the hadronic VP contributions have been added linearly. Compared to  $a_e^{\text{had}}(\text{NT12}) = (167.8 \pm 1.4) \times 10^{-14}$  in [17], the mean value found in this work is outside the quoted error given in [17]. However, it should be noted that no determination of the NNLO hadronic VP contributions was available for [17], whereas in this work the addition of  $a_e^{\text{had, NNLO VP}} = (2.80 \pm 0.01) \times 10^{-14}$  constitutes, similar to the case of the muon, a significant additional correction.

The EW contributions,  $a_e^{\text{EW}} = (3.053 \pm 0.023) \times 10^{-14}$ , are also taken from [47]. For the QED contributions, there are now two options depending on the choice for the value of  $\alpha$ .<sup>5</sup> As described in Section 1, the use of the measurement of  $\alpha$  from Rb atomic interferometry [13] or Cs atomic interferometry [14] leads to an interesting comparison with  $a_e^{\text{exp}}$ . For each case, the

<sup>4</sup>During the KNT18 analysis, the authors of [24] kindly repeated their analysis with the KNT18 data compilation and found negligible changes with respect to their published result.

<sup>5</sup>For the contributions from all the other sectors of the SM, the changes from the choice of  $\alpha$  are negligible.

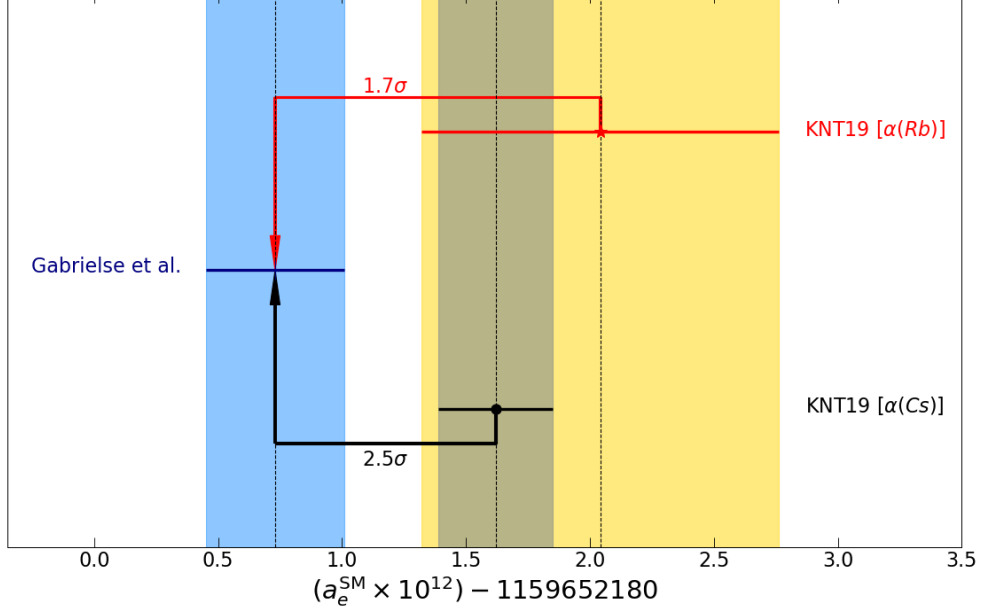


Figure 7: A comparison of the evaluations of  $a_e^{\text{SM}}$  as determined in this work with the experimental measurement by Gabrielse *et al.* [10], the uncertainty of which is given by the light blue band. The red marker and yellow band denote the determination of  $a_e^{\text{SM}}$  using  $\alpha_{\text{Rb}}$ , whilst the black marker and grey band denote the determination of  $a_e^{\text{SM}}$  using  $\alpha_{\text{Cs}}$  (for the values see equations (3.5) or Table 2).

values of  $a_e^{\text{QED}}$  are

$$\begin{aligned} a_e^{\text{QED}}(\alpha_{\text{Rb}}) &= (115965218030.9 \pm 72.0) \times 10^{-14} \text{ [11]}, \\ a_e^{\text{QED}}(\alpha_{\text{Cs}}) &= (115965217988.7 \pm 23.0) \times 10^{-14} \text{ [14]}. \end{aligned} \quad (3.4)$$

Using these and the contributions from the EW and hadronic sectors, the SM predictions for  $a_e$  are found here to be

$$\begin{aligned} a_e^{\text{SM}}(\alpha_{\text{Rb}}) &= (1159652182.042 \pm 0.72) \times 10^{-12}, \\ a_e^{\text{SM}}(\alpha_{\text{Cs}}) &= (1159652181.620 \pm 0.23) \times 10^{-12}. \end{aligned} \quad (3.5)$$

The comparison of these results with the experimental measurement of  $a_e$  [10] is given in Table 2 and shown in Figure 7. The values of the deviation between theory and experiment of  $\Delta a_e(\alpha_{\text{Rb}}) = (-1.31 \pm 0.77) \times 10^{-12}$  ( $1.7\sigma$ ) and  $\Delta a_e(\alpha_{\text{Cs}}) = (-0.89 \pm 0.36) \times 10^{-12}$  ( $2.5\sigma$ ) confirm the findings in [11] and [14], respectively.

### 3.2 The anomalous magnetic moment of the muon, $a_\mu$

For the hadronic VP contribution to  $a_\mu$ , at LO this analysis finds

$$\begin{aligned} a_\mu^{\text{had, LO VP}} &= (692.78 \pm 1.21_{\text{stat}} \pm 1.97_{\text{sys}} \pm 0.21_{\text{vp}} \pm 0.70_{\text{fsr}}) \times 10^{-10} \\ &= (692.78 \pm 2.42_{\text{tot}}) \times 10^{-10}, \end{aligned} \quad (3.6)$$

and the NLO contributions are determined here to be

$$\begin{aligned} a_\mu^{\text{had, NLO VP}} &= (-9.83 \pm 0.01_{\text{stat}} \pm 0.03_{\text{sys}} \pm 0.01_{\text{vp}} \pm 0.02_{\text{fsr}}) \times 10^{-10} \\ &= (-9.83 \pm 0.04_{\text{tot}}) \times 10^{-10}. \end{aligned} \quad (3.7)$$

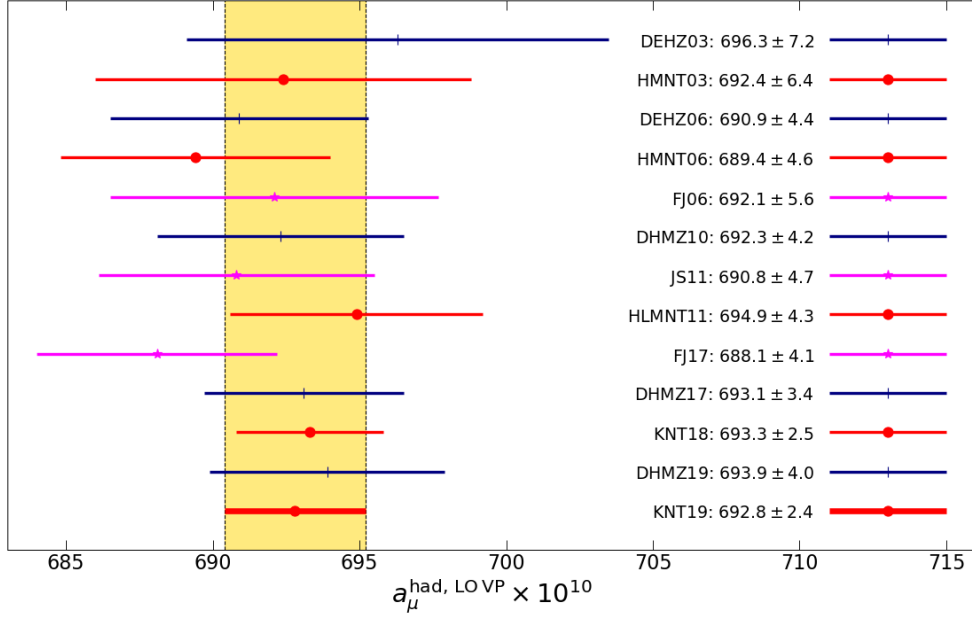


Figure 8: Comparison of recent and previous evaluations of  $a_\mu^{\text{had, LO VP}}$  determined from  $e^+e^- \rightarrow \text{hadrons}$  cross section data. The analyses listed in chronological order are: DEHZ03 [48], HMNT03 [22], DEHZ06 [49], HMNT06 [39], FJ06 [50], DHMZ10 [51], JS11 [52], HLMNT11 [40], FJ17 [53], DHMZ17 [54], KNT18 [1] and DHMZ19 [37]. The prediction from this work is listed as KNT19 and defines the (yellow) uncertainty band shown for the comparison with the other analyses.

These results are consistent with the KNT18 analysis. At LO, the integral over the hadronic  $R$ -ratio determined in [1] resulted in  $a_\mu^{\text{had, LO VP}}(\text{KNT18}) = (693.26 \pm 2.46) \times 10^{-10}$ . Comparing this with equation (3.6), the reduction in the mean value comes entirely from the updated treatment of the  $\omega$  resonance in the  $\pi^+\pi^-\pi^0$  channel described in Section 2.2. This change counteracts the small increase in the mean value from the  $\pi^+\pi^-$  channel due to the inclusion of the CLEO-c data [25] detailed in Section 2.1, as well as the very small increase due to the newly included channels reported in Section 2.3. The marginal decrease in the overall uncertainty is also due to the inclusion of the CLEO-c data [25], which as explained previously has caused a small decrease in the local  $\chi^2$  error inflation of the dominant two-pion contribution. A comparison of this result with similar evaluations of  $a_\mu^{\text{had, LO VP}}$  determined from  $e^+e^- \rightarrow \text{hadrons}$  cross section data is shown in Figure 8. It is important to note that there is clear stability and overall agreement between the different analyses/groups over the consecutive years, despite contrasting choices the different groups have made concerning how to treat the hadronic cross section data, where to use perturbative QCD (pQCD) instead of data and the application of other possible theoretical constraints.<sup>6</sup>

Combining the results (3.6) and (3.7) with the NNLO corrections,  $a_\mu^{\text{had, NNLO VP}} = (1.24 \pm$

<sup>6</sup> The most recent update from DHMZ19 has a larger uncertainty compared to that of DHMZ17, since DHMZ19 have included an additional error to account for the difference they obtain for  $a_\mu^{\pi^+\pi^-}$  when discarding either the KLOE or the BaBar data. As the KNT  $\pi^+\pi^-$  data combination benefits from stronger constraints imposed by the correlated uncertainties, the difference observed in  $a_\mu^{\pi^+\pi^-}$  when discarding the data from either experiment is less severe. Therefore, and remembering also that data tensions are quantitatively accounted for in the resulting cross section by the local  $\chi^2$  error inflation, no additional uncertainty for  $a_\mu$  is applied in this analysis.

$0.01) \times 10^{-10}$  [24], the total hadronic VP contribution to  $a_\mu$  is estimated to be

$$a_\mu^{\text{had, VP}} = (684.19 \pm 2.38_{\text{tot}}) \times 10^{-10}, \quad (3.8)$$

where, as in the case of the electron, the errors have been added linearly due to the full correlation between the  $R$ -ratio input for the three contributions. When considering the SM prediction, in the case of the muon ( $l = \mu$ ), the other contributions in equation (1.1) require reconsideration. In contrast to the case of the electron, the muon is, at the current level of accuracy, not sensitive to the choice of either  $\alpha(\text{Rb})$  or  $\alpha(\text{Cs})$ , or the updated five-loop QED contributions from [11]. Hence the value of the QED contributions, to the accuracy needed and quoted here, is unchanged at  $a_\mu^{\text{QED}} = (11658471.90 \pm 0.01) \times 10^{-10}$  [11, 55]. For the EW contributions, the value chosen here is also the same as in [1]. However, it should be noted that an independent numerical evaluation of the two-loop EW contributions was recently performed [56], resulting in an estimate of the total EW contributions of  $a_\mu^{\text{EW}} = (15.29 \pm 0.10) \times 10^{-10}$ . This is consistent with the previously chosen value of  $a_\mu^{\text{EW}} = (15.36 \pm 0.10) \times 10^{-10}$  [57] and therefore no adjustment is made for this analysis.

For the hadronic LbL sector, in [1] the commonly quoted ‘Glasgow consensus’ estimate of  $a_\mu^{\text{had, LbL}}$  (‘Glasgow consensus’) =  $(10.5 \pm 2.6) \times 10^{-10}$  [58] was used, adjusted for a re-evaluation of the contribution to  $a_\mu^{\text{had, LbL}}$  due to axial exchanges [59–61]. This led to  $a_\mu^{\text{had, LbL}} = (9.8 \pm 2.6) \times 10^{-10}$  [61] being adopted for the KNT18 analysis. Since that time, the progress in determining  $a_\mu^{\text{had, LbL}}$  using dispersive approaches (where dispersion relations are formulated that allow for the determination of the hadronic LbL contributions from experimental data) has been significant.<sup>7</sup> These determinations are of particular interest for this analysis, as the fundamental approach to this work (and the works preceding it [1, 22, 39, 40]) is that any estimates given be as model-independent and/or as data-driven as possible. With the contributions to the ‘Glasgow consensus’ estimate having been solely determined through model-dependent approaches, moving towards data-based evaluations of the hadronic LbL contributions is consistent with the general methodology of this undertaking.

Those hadronic LbL contributions that have been determined by dispersive techniques are the pseudoscalar poles ( $\pi^0, \eta, \eta'$ ) [62–64], the pion/kaon-box contributions [9, 65] and the  $S$ -wave  $\pi\pi$  rescattering contributions [65, 66]. In addition, a new analysis of (longitudinal) short distance constraints has very recently become available [67, 68], complementing the dispersive determination of the pseudoscalar contributions. The values for these contributions and their counterparts from the ‘Glasgow consensus’ estimate are shown in Table 3, where the estimate of the pseudoscalar contributions of the ‘Glasgow consensus’ already contains short distance contributions. With the aim to strive for a more model-independent approach, the value for  $a_\mu^{\text{had, LbL}}$  in this work is taken as the sum of the contributions determined via dispersive approaches, the new estimates of short distance and charm quark corrections, plus the sum of the contributions from scalars, tensors and axial-vectors remaining from the original ‘Glasgow consensus’ estimate.<sup>8</sup> This results in a value for the total hadronic LbL contribution of  $a_\mu^{\text{had, LbL}} = (9.34 \pm 2.92) \times 10^{-10}$ , where the errors from the individual contributions have been summed linearly. This provides

<sup>7</sup>This advancement has been largely influenced by the efforts of the Muon  $g - 2$  Theory Initiative [9] and the commendable work and successes of the groups within it, which have formed the basis for the following choices for  $a_\mu^{\text{had, LbL}}$  made in this work.

<sup>8</sup>Note that the adjustments of the axial contributions mentioned above and adopted in [1], have recently been found not justified, see [69], hence the estimate for the axial contributions from the original ‘Glasgow consensus’ is used here.

Contribution	‘Glasgow consensus’ [58]	Dispersive evaluations
$\pi^0, \eta, \eta'$ -poles	$114 \pm 13$	$93.8 \pm 4.0$ [62–64]
$\pi/K$ -box	$-19 \pm 19$	$-16.4 \pm 0.2$ [9, 65]
$S$ -wave $\pi\pi$ rescattering	-	$-8 \pm 1$ [65, 66]
Short-distance contributions	[Part of $\pi^0, \eta, \eta'$ -poles]	$13 \pm 6$ [67, 68]
Charm contributions	2.3	$3 \pm 1$ [67, 68]
Scalars & Tensors		$-7 \pm 7$
Axial-vectors		$15 \pm 10$
Total	$105 \pm 26$	$93.4 \pm 29.2$

Table 3: Comparison of the contributions to  $a_\mu^{\text{had, LbL}}$  from the ‘Glasgow consensus’ estimate and from recent evaluations mainly based on dispersive approaches. The single column results from the scalars, tensors and axial-vectors originate from the ‘Glasgow consensus’ estimate. The total uncertainty for the value including the dispersive evaluations is determined via the conservative linear sum of the errors of the individual contributions. All results are given as  $a_\mu^{\text{had, LbL}} \times 10^{11}$ .

SM contribution	$a_\mu \times 10^{10}$
QED	$11658471.90 \pm 0.01$ [11]
EW	$15.36 \pm 0.10$ [57]
had LO VP	$692.78 \pm 2.42$
had NLO VP	$-9.83 \pm 0.04$
had NNLO VP	$1.24 \pm 0.01$ [24]
had LO LbL	$9.34 \pm 2.92$
had NLO LbL	$0.30 \pm 0.20$ [70]
Theory total	$11659181.08 \pm 3.78$
Experiment	$11659209.10 \pm 6.33$ [5]
$\Delta a_\mu$	$28.02 \pm 7.37$ ( $3.80\sigma$ )

Table 4: Summary of the contributions to  $a_\mu^{\text{SM}}$ .

a conservative estimate of the overall uncertainty and also accounts for currently unavailable transverse short distance constraints, which are estimated to be sub-leading.

The values for the contributions from all the individual sectors of the SM chosen in this analysis are summarised in Table 4. Summing these contributions together results in an updated SM prediction of the anomalous magnetic moment of the muon of

$$a_\mu^{\text{SM}} = (11\,659\,181.08 \pm 3.78) \times 10^{-10}, \quad (3.9)$$

where the uncertainty is determined from the uncertainties of the individual SM contributions added in quadrature. This value deviates from the current experimental measurement [5] by

$$\Delta a_\mu = (28.02 \pm 7.37) \times 10^{-10}, \quad (3.10)$$

corresponding to a muon  $g - 2$  discrepancy of  $3.8\sigma$ . This result is compared with other determinations of  $a_\mu^{\text{SM}}$  in Figure 9. The value for  $a_\mu^{\text{SM}}$  in equation (3.9) has decreased by  $0.96 \times 10^{-10}$

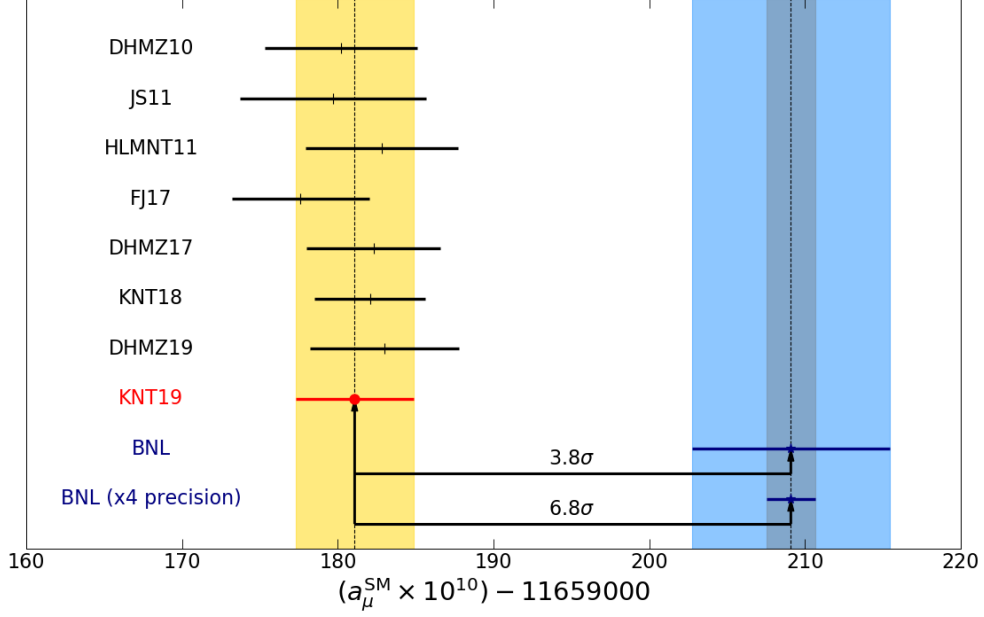


Figure 9: A comparison of recent and previous evaluations of  $a_\mu^{\text{SM}}$ . The analyses listed in chronological order are: DHMZ10 [51], JS11 [52], HLMNT11 [40], FJ17 [53] and DHMZ17 [54], KNT18 [1] and DHMZ19 [37]. The prediction from this work is listed as KNT19, which defines the uncertainty band that other analyses are compared to. The current uncertainty on the experimental measurement [2–5] is given by the light blue band. The light grey band represents the hypothetical situation of the new experimental measurement at Fermilab yielding the same mean value for  $a_\mu^{\text{exp}}$  as the BNL measurement, but achieving the projected four-fold improvement in its uncertainty [6].

compared to the KNT18 analysis [1]. This change comes, in nearly equal parts, from the reduction in the mean value of  $a_\mu^{\text{had, LO VP}}$  and the new estimate of  $a_\mu^{\text{had, LbL}}$  in this work. The increase in the uncertainty with respect to [1] comes from the increase in the error of  $a_\mu^{\text{had, LbL}}$  owing to the changes in the estimate of this contribution discussed previously. Together, these have resulted in the increased discrepancy from  $3.7\sigma$  in the KNT18 analysis to  $3.8\sigma$  in this work.

### 3.3 The anomalous magnetic moment of the tau lepton, $a_\tau$

In the case of the  $\tau$ , the determination of the LO hadronic VP contributions yields

$$\begin{aligned} a_\tau^{\text{had, LO VP}} &= (332.81 \pm 0.47_{\text{stat}} \pm 1.09_{\text{sys}} \pm 0.17_{\text{vp}} \pm 0.69_{\text{fsr}}) \times 10^{-8} \\ &= (332.81 \pm 1.39_{\text{tot}}) \times 10^{-8}, \end{aligned} \quad (3.11)$$

whilst at NLO they are found to be

$$\begin{aligned} a_\tau^{\text{had, NLO VP}} &= (7.85 \pm 0.01_{\text{stat}} \pm 0.03_{\text{sys}} \pm 0.01_{\text{vp}} \pm 0.02_{\text{fsr}}) \times 10^{-8} \\ &= (7.85 \pm 0.04_{\text{tot}}) \times 10^{-8}. \end{aligned} \quad (3.12)$$

Note that in the case of the  $\tau$ , the total NLO contributions are positive, while they are negative for the electron and muon, and any estimate based on a naive mass-scaling of the result for the muon would fail completely. The results for  $a_\tau^{\text{had, LO VP}}$  from the individual hadronic channels are given in Table 1. Comparing with the evaluation in [19], which resulted in  $a_\tau^{\text{had, LO VP}} =$



SM contribution	$a_\tau$
QED	$(117324.0 \pm 2.0) \times 10^{-8}$ [19]
EW	$(47.4 \pm 0.5) \times 10^{-8}$ [19]
had LO VP	$(332.8 \pm 1.4) \times 10^{-8}$
had NLO VP	$(7.9 \pm 0.0) \times 10^{-8}$
had LbL	$(5.0 \pm 3.0) \times 10^{-8}$ [19]
Theory total	$(117717.1 \pm 3.9) \times 10^{-8}$
Experiment	$-0.018 \pm 0.017$ [18]
$\Delta a_\tau$	$-0.019 \pm 0.017$ ( $-1.1\sigma$ )

Table 5: Summary of the contributions to  $a_\tau^{\text{SM}}$ .

$(337.5 \pm 3.7) \times 10^{-8}$ , and  $a_\tau^{\text{had,NLO VP}} = (7.6 \pm 0.2) \times 10^{-8}$  obtained already in [23], there is consistency between the mean values found in the different analyses. However, there is a large reduction in the error in this work which is mainly due to the abundance of precise new data since [19]. Utilising the values from [19] for the QED, EW and hadronic LbL contributions (listed in Table 5), the updates to the hadronic VP contributions result in a SM prediction for the anomalous magnetic moment of the tau lepton of

$$a_\tau^{\text{SM}} = (117717.1 \pm 3.9) \times 10^{-8}. \quad (3.13)$$

With the uncertainties of the hadronic VP contributions significantly improved, the uncertainty of  $a_\tau^{\text{SM}}$  is now dominated by the hadronic LbL contributions, which account for  $\sim 60\%$  of the total error. However, it should be noted that the QED contributions, at  $\sim 26\%$  of the total error, are now less precise than the hadronic VP contributions. As explained in [19], the entire error  $\delta a_\tau^{\text{QED}} \sim 2 \times 10^{-8}$  is assigned as the uncertainty due to the missing contributions at four-loop (and beyond), and are crudely estimated from logarithmically enhanced terms expected at four-loop level. This indicates that a calculation of  $a_\tau^{\text{QED}}$  at four loops would significantly improve the determination of  $a_\tau^{\text{SM}}$ .

Although, as stated in Section 1, the precision of the current experimental measurement of  $a_\tau^{\text{exp}} = -0.018(17)$  [18] makes a meaningful comparison between theory and experiment futile, this analysis confirms a difference  $\Delta a_\tau = a_\tau^{\text{exp}} - a_\tau^{\text{SM}}$  at the level of  $1\sigma$  as found in [18]. While at present there seems little prospect for an experiment dedicated to measuring  $a_\tau$ , it is not imperceivable to imagine that this might become possible in the future. Indeed, the additional potential for new physics discoveries due to the higher mass scale of the  $\tau$  compared to the electron or the muon make this an interesting consideration.

### 3.4 Determination of $\alpha(M_Z^2)$

The running (scale dependent) QED coupling,  $\alpha(q^2)$ , is determined via  $\alpha(q^2) = \alpha/(1 - \Delta\alpha_{\text{had}}(q^2) - \Delta\alpha_{\text{lep}}(q^2))$ , where the contributions to the running are separated into hadronic (had) and leptonic (lep) components. Of the three fundamental EW parameters of the SM (the Fermi constant  $G_F$ ,  $M_Z$  and  $\alpha(M_Z^2)$ ), the effective QED coupling at the  $Z$  boson mass,  $\alpha(M_Z^2)$ , is the least precisely known, where the uncertainties from the non-perturbative, hadronic contributions limit the accuracy of EW precision fits. The five-flavour (all quark flavours except the top quark which can be treated perturbatively) contributions to  $\alpha(M_Z^2)$  are determined from the dispersion

Analysis	$\Delta\alpha_{\text{had}}^{(5)}(M_Z^2) \times 10^4$	$\alpha^{-1}(M_Z^2)$
DHMZ10 [51]	$275.59 \pm 1.04$	$128.952 \pm 0.014$
HLMNT11 [40]	$276.26 \pm 1.38$	$128.944 \pm 0.019$
FJ17 [47]	$277.38 \pm 1.19$	$128.919 \pm 0.022$
DHMZ17 [54]	$276.00 \pm 0.94$	$128.947 \pm 0.012$
KNT18	$276.11 \pm 1.11$	$128.946 \pm 0.015$
DHMZ19 [37]	$276.10 \pm 1.00$	$128.946 \pm 0.013$
KNT19 [This work]	$276.09 \pm 1.12$	$128.946 \pm 0.015$

Table 6: Comparison of recent and previous evaluations of  $\Delta\alpha_{\text{had}}^{(5)}(M_Z^2)$  determined from  $e^+e^- \rightarrow$  hadrons cross section data and the corresponding results for  $\alpha^{-1}(M_Z^2)$ .

relation

$$\Delta\alpha_{\text{had}}^{(5)}(M_Z^2) = -\frac{\alpha M_Z^2}{3\pi} \text{P} \int_{s_{th}}^{\infty} ds \frac{R(s)}{s(s - M_Z^2)}, \quad (3.14)$$

where P indicates the principal value of the integral. Using the updated compilation for  $R(s)$  from this work, and perturbative QCD for energies  $\sqrt{s} > 11.199$  GeV (above the thresholds for all five quark flavours), this data-driven evaluation gives the result

$$\begin{aligned} \Delta\alpha_{\text{had}}^{(5)}(M_Z^2) &= (276.09 \pm 0.26_{\text{stat}} \pm 0.68_{\text{sys}} \pm 0.14_{\text{vp}} \pm 0.83_{\text{fsr}}) \times 10^{-4} \\ &= (276.09 \pm 1.12_{\text{tot}}) \times 10^{-4}. \end{aligned} \quad (3.15)$$

From this, the total value of the QED coupling at the Z boson mass is

$$\begin{aligned} \alpha^{-1}(M_Z^2) &= \left(1 - \Delta\alpha_{\text{lep}}(M_Z^2) - \Delta\alpha_{\text{had}}^{(5)}(M_Z^2) - \Delta\alpha_{\text{top}}(M_Z^2)\right) \alpha^{-1} \\ &= 128.946 \pm 0.015, \end{aligned} \quad (3.16)$$

updating the result from [1]. As in [1], the leptonic contribution is  $\Delta\alpha_{\text{lep}}(M_Z^2) = (314.979 \pm 0.002) \times 10^{-4}$  [71, 72]. The contribution from the top quark is updated from [73, 74] by using  $m_t = 172.9(0.4)$  GeV,  $\alpha_s(M_Z) = 0.1181(11)$  [2] and by including the contributions from  $\mathcal{O}(\alpha_s^0 m_Z^6/m_t^6)$  and  $\mathcal{O}(\alpha_s^1 m_Z^6/m_t^6)$  terms which were neglected in [74]. This results in  $\Delta\alpha_{\text{top}}(M_Z^2) = (-0.7201 \pm 0.0037) \times 10^{-4}$ . A comparison with previous, largely data-driven determinations of  $\Delta\alpha_{\text{had}}^{(5)}(M_Z^2)$  and  $\alpha^{-1}(M_Z^2)$  is given in Table 6.

### 3.5 The hyperfine splitting of muonium, $\Delta\nu_{\text{Mu}}^{\text{had, VP}}$

For many years, precision measurements of the ground-state hyperfine splitting (HFS) of muonium  $\Delta\nu_{\text{Mu}}$  served as a rigorous test of QED. Today, it still provides the best approach for determining the value of the electron-to-muon mass ratio and, therefore, the muon mass. As, like with the lepton  $g - 2$ ,  $\Delta\nu_{\text{Mu}}$  is sensitive to quantum effects, any differences in the comparison of experimental and theoretical determinations could be an indication of new physics. The current most precise experimental measurements of  $\Delta\nu_{\text{Mu}}$  [75, 76] result in

$$\Delta\nu_{\text{Mu}}^{\text{exp}} = (4\,463\,302\,776 \pm 51) \text{ Hz}. \quad (3.17)$$

With the most recent of these measurements having been performed more than 20 years ago, the MuSEUM experiment at J-PARC is currently in the process of measuring the HFS of muonium

(and the electron-to-muon mass ratio) with an aim to reduce the uncertainty in equation (3.17) by an order of magnitude [77].

The theoretical prediction,  $\Delta\nu_{\text{Mu}}^{\text{SM}}$ , as given by CODATA 2014 [78]<sup>9</sup>, is

$$\Delta\nu_{\text{Mu}}^{\text{SM}}(\text{CODATA}) = (4\,463\,302\,868 \pm 271) \text{ Hz} . \quad (3.18)$$

Although the HFS of muonium is mainly QED dominated, it receives higher-order contributions from the EW and hadronic sectors. In the case of the hadronic contributions, the hadronic LO VP contributions are dominant, whilst the hadronic LbL contributions are negligible compared to the current level of precision ( $\Delta\nu_{\text{Mu}}^{\text{had, LbL}} \simeq 0.0065(10) \text{ Hz}$  [78,80]). The CODATA determination given in equation (3.18) currently utilises the value for the hadronic LO VP contributions that was determined in the NT12 analysis preceding this work [17], which found

$$\Delta\nu_{\text{Mu}}^{\text{had, VP}}(\text{NT12}) = (232.68 \pm 1.44) \text{ Hz} . \quad (3.19)$$

These contributions can be determined via the dispersion integral

$$\Delta\nu_{\text{Mu}}^{\text{had, VP}} = \frac{1}{2\pi^3} \frac{m_e}{m_\mu} \nu_F \int_{m_{\pi^0}^2}^{\infty} ds K_{\text{Mu}}(s) \sigma_{\text{had}, \gamma}^0(s) . \quad (3.20)$$

Here,  $\nu_F$  denotes the so-called Fermi energy,

$$\nu_F = \frac{16}{3} R_\infty \alpha^2 \frac{m_e}{m_\mu} \left[ 1 + \frac{m_e}{m_\mu} \right]^{-3} , \quad (3.21)$$

where  $R_\infty$  is the Rydberg constant. The kernel function  $K_{\text{Mu}}(s)$  is described in detail in [17].

Now utilising the compilation of the hadronic cross section determined in this work (see Section 2), the updated value for the hadronic VP contributions to the ground-state HFS of muonium are found to be

$$\begin{aligned} \Delta\nu_{\text{Mu}}^{\text{had, VP}} &= (232.04 \pm 0.38_{\text{stat}} \pm 0.66_{\text{sys}} \pm 0.08_{\text{vp}} \pm 0.27_{\text{fsr}}) \text{ Hz} \\ &= (232.04 \pm 0.82_{\text{tot}}) \text{ Hz} . \end{aligned} \quad (3.22)$$

Here, a noticeable mean value reduction and an uncertainty reduction of  $\sim 43\%$  compared to equation (3.19) are observed, which is in accordance with the same trends seen in the development of the corresponding determinations of  $a_\mu$  over the same period. Adjusting the theoretical prediction in equation (3.18) for this value results in

$$\Delta\nu_{\text{Mu}}^{\text{SM}} = (4\,463\,302\,867 \pm 271) \text{ Hz} , \quad (3.23)$$

which, despite the noticeable changes in  $\Delta\nu_{\text{Mu}}^{\text{had, VP}}$  between this work and the previous analysis, highlights the minimal impact of the hadronic contributions to this observable compared to the dominant QED contributions.

---

<sup>9</sup>Note that in [79] it was claimed that the uncertainty in equation (3.18) is underestimated by a factor of  $\sim 1/2$  due to the implicit assumption that there is no new physics beyond the SM in relations used by the CODATA estimate. The theoretical (th) prediction in [79] reads  $\Delta\nu_{\text{Mu}}^{\text{th}} = (4\,463\,302\,872 \pm 515) \text{ Hz}$ .

## 4 Conclusions and future prospects

This analysis, KNT19, has presented updated evaluations of the hadronic vacuum polarisation contributions to the anomalous magnetic moment of the electron ( $a_e^{\text{had,VP}}$ ), muon ( $a_\mu^{\text{had,VP}}$ ) and tau lepton ( $a_\tau^{\text{had,VP}}$ ), to the ground-state hyperfine splitting of muonium ( $\Delta\nu_{\text{Mu}}^{\text{had,VP}}$ ), and has also updated the value of the hadronic contributions to the running of the QED coupling at the scale of the mass of the  $Z$  boson ( $\Delta\alpha_{\text{had}}(M_Z^2)$ ). These quantities are calculated using the hadronic  $R$ -ratio, obtained from a compilation of all available  $e^+e^- \rightarrow \text{hadrons}$  cross section data. In this work, the data compilation has been updated from the determination in [1], accounting for new measurements. In the dominant  $\pi^+\pi^-$  channel, the inclusion of the CLEO-c data [25] has increased the mean value slightly and marginally improved the uncertainty of  $a_\mu^{\pi^+\pi^-}$ . In the  $\pi^+\pi^-\pi^0$  channel, adjustments have been made to the treatment of the narrow  $\omega$  resonance, which is now integrated over using a quintic polynomial interpolation in order to avoid an overestimation of the cross section from a linear interpolation that was recently noted in [38]. This has reduced the mean value of  $a_\mu^{\pi^+\pi^-\pi^0}$  by  $\sim 1 \times 10^{-10}$  and, in turn, contributed to a significant reduction of the mean value of  $a_\mu^{\text{SM}}$  in this work, although it is important to note that all estimates from this analysis are consistent with those given in [1]. In addition, other new measurements have been included which have removed the need to rely on isospin relations to estimate cross sections in three sub-leading channels, where in each case the new data agree well with the predictions of the KNT18 analysis.

The resulting hadronic  $R$ -ratio has been used as input into dispersion relations to determine  $a_l^{\text{had,VP}}$  ( $l = e, \mu, \tau$ ) at LO and NLO,  $\Delta\alpha_{\text{had}}(M_Z^2)$  and  $\Delta\nu_{\text{Mu}}^{\text{had,VP}}$ . This work has found  $\Delta\alpha_{\text{had}}^{(5)}(M_Z^2) = (276.09 \pm 1.12_{\text{tot}}) \times 10^{-4}$  which has yielded a value for the QED coupling at the  $Z$  boson mass of  $\alpha^{-1}(M_Z^2) = 128.946 \pm 0.015$ , which is consistent with [1]. For the hadronic VP contributions to the ground-state hyperfine splitting of muonium, the new data compilation gives  $\Delta\nu_{\text{Mu}}^{\text{had,VP}} = (232.04 \pm 0.82_{\text{tot}})$  Hz, which is consistent with the previous determination of this quantity in [17], but constitutes a significant uncertainty reduction of  $\sim 43\%$ . A similar error reduction has been observed in the determination of the anomalous magnetic moment of the electron compared to [17], with this analysis finding  $a_e^{\text{had,LO VP}} = (186.08 \pm 0.66_{\text{tot}}) \times 10^{-14}$ . This, coupled with new estimates for the NLO contributions, translates to differences between experiment and theory of  $\Delta a_e(\alpha_{\text{Rb}}) = (-1.312 \pm 0.773) \times 10^{-12}$  ( $1.7\sigma$ ) and  $\Delta a_e(\alpha_{\text{Cs}}) = (-0.890 \pm 0.362) \times 10^{-12}$  ( $2.5\sigma$ ), depending on whether the QED contributions are determined using  $\alpha$  measured via Rb or Cs atomic interferometry. For the muon  $g-2$ , the new KNT19 analysis gives  $a_\mu^{\text{had,LO VP}} = (692.78 \pm 2.42_{\text{tot}}) \times 10^{-10}$  and  $a_\mu^{\text{had,NLO VP}} = (-9.83 \pm 0.04_{\text{tot}}) \times 10^{-10}$ . New choices in this work for the hadronic LbL contributions based on recent results from dispersive approaches (which have already significantly consolidated the ‘Glasgow consensus’), coupled with the contributions from the other sectors of the SM, have resulted in a new estimate for the Standard Model prediction of  $a_\mu^{\text{SM}} = (11\,659\,181.08 \pm 3.78) \times 10^{-10}$ , which deviates from the current experimental measurement by  $3.8\sigma$ . In the case of the  $\tau$ , the value at LO is  $a_\tau^{\text{had,LO VP}} = (332.81 \pm 1.39_{\text{tot}}) \times 10^{-8}$ , consistent with the value found in [19], but with an uncertainty that is smaller by  $\sim 62\%$ . Unfortunately, the current experimental bounds of the measured value of  $a_\tau$  are not stringent enough to draw any strong conclusions from the comparison between experiment and theory.

It is interesting to compare the values and uncertainties of  $a_l^{\text{had,LO VP}}$  and  $a_l^{\text{SM}}$  of the different leptons, which are shown in Table 7. Here, especially in the case of the hadronic contributions, the difference in the resulting magnitudes of these values due to lepton mass-scaling arguments is evident. Indeed, in the most extreme example, the value of  $a_l^{\text{had,LO VP}}$  is

Lepton flavour, $l$	$a_l^{\text{had, LO VP}} \times 10^7$	$a_l^{\text{SM}} \times 10^7$
$e$	0.00001861(7)	11596.52182042(720)
$\mu$	0.69278(242)	11659.18108(378)
$\tau$	33.281(139)	11771.71(39)

Table 7: Comparison of the contributions to  $a_l^{\text{had, LO VP}}$  and  $a_l^{\text{SM}}$  as determined in this work. All results are presented in units of  $a_l \times 10^7$  in order to compare the relevant magnitudes and precision of the various contributions. In this instance, the value of  $a_e^{\text{SM}}$  corresponds to  $a_e^{\text{QED}}$  determined using  $\alpha_{\text{RB}}$ .

$\mathcal{O}(10^6)$  times larger for the  $\tau$  than for the electron. For  $a_l^{\text{SM}}$ , the most striking difference is in the level of the precision between the different leptons. The electron, being less sensitive to hadronic effects than the muon or the  $\tau$ , is by far the most precise. However, the larger uncertainty of  $a_\tau^{\text{SM}}$  compared to  $a_\mu^{\text{SM}}$  is not solely due to hadronic contributions (where, for the muon, the hadronic LbL estimates are more accurate than for the  $\tau$ ). Instead, as noted in Section 3.3, the uncertainty assigned due to the missing four-loop contributions is a main cause of this disparity and could be improved through the calculation of  $a_\tau^{\text{QED}}$  at four-loop order.

With the tantalising prospect of new experimental measurements of  $a_\mu$  from Fermilab in the near future, and later from J-PARC, the predictions of  $a_\mu^{\text{had, VP}}$  and  $a_\mu^{\text{SM}}$  have been re-examined in detail and found to be robust. The opportunity to further improve the hadronic VP contributions estimated by dispersive approaches (as in this analysis) largely rests on new hadronic cross section measurements. For the  $\pi^+\pi^-$  channel, new measurements currently under analysis from the CMD-3, SND and BaBar experiments are eagerly awaited. Although these measurements are important in terms of improving the overall precision of  $a_\mu^{\text{had, VP}}$ , it is hoped that they will help to resolve the lingering deviation between the KLOE [28–31] and BaBar [32] measurements, which drive the data tensions in  $a_\mu^{\pi^+\pi^-}$ . In addition, expected data for the  $\pi^+\pi^-\pi^0$ ,  $\pi^+\pi^-\pi^0\pi^0$  and the inclusive channels, will be very beneficial. In preparation for the new experimental measurements of  $a_\mu$ , the efforts of the Muon  $g-2$  Theory Initiative [9] (and the groups within it) have already led to impressive achievements with regards to advancing the determinations of the hadronic VP and hadronic LbL contributions. Of great interest are the results from lattice QCD, which already provide first-principles cross checks of the now very precise data-driven estimates for the hadronic contributions to  $a_\mu^{\text{SM}}$ . These are expected to become competitive with the current determinations within the next few years. Given the continued advancements in the theoretical predictions of  $a_\mu$ , coupled with the substantial progress of the experimental community, the study of the muon anomalous magnetic moment has never been better placed to severely constrain many scenarios for new physics beyond the SM, or, should the muon  $g-2$  discrepancy become fully established, to claim a discovery of new physics.

## Acknowledgements

We would like to thank Martin Hoferichter, Bai-Long Hoid, Bastian Kubis, the DHMZ group (Michel Davier, Andreas Hoecker, Bogdan Malaescu and Zhiqing Zhang) and, in general, *The Muon  $g-2$  Theory Initiative* and the Muon  $g-2$  collaboration for numerous useful discussions. Alex Keshavarzi would like to thank Tsutomu Mibe and the KEK Laboratory for hosting him during part of the writing of this paper.

The work of Alex Keshavarzi is supported in-part by STFC under the consolidated grant ST/S000925/1. This manuscript has been authored by an employee of The University of Mississippi (A.K.), supported in-part by the U.S. Department of Energy Office of Science, Office of High Energy Physics, award DE-SC0012391. This document was prepared using the resources of the Fermi National Accelerator Laboratory (Fermilab), a U.S. Department of Energy, Office of Science, HEP User Facility. Fermilab is managed by Fermi Research Alliance, LLC (FRA), acting under Contract No. DE-AC02-07CH11359. The work of Daisuke Nomura is supported by JSPS KAKENHI grant number JP17H01133. The work of Thomas Teubner is supported by STFC under the consolidated grants ST/P000290/1 and ST/S000879/1.

## References

- [1] A. Keshavarzi, D. Nomura and T. Teubner, *Phys. Rev. D* **97** (2018) 114025.
- [2] M. Tanabashi *et al.* (Particle Data Group), *Phys. Rev. D* **98** (2018) 030001 and 2019 update.
- [3] G. W. Bennett *et al.* [Muon g-2 Collaboration], *Phys. Rev. Lett.* **89** (2002) 101804 [Erratum: *Phys. Rev. Lett.* **89** (2002) 129903].
- [4] G. W. Bennett *et al.* [Muon g-2 Collaboration], *Phys. Rev. Lett.* **92** (2004) 161802.
- [5] G. W. Bennett *et al.* [Muon g-2 Collaboration], *Phys. Rev. D* **73** (2006) 072003.
- [6] J. Grange *et al.* [Muon g-2 Collaboration], arXiv:1501.06858 [physics.ins-det].
- [7] A. Keshavarzi [Muon g-2 Collaboration], *EPJ Web Conf.* **212** (2019) 05003.
- [8] M. Abe *et al.*, *PTEP* **2019** (2019) 053C02.
- [9] *The Muon g – 2 Theory Initiative*,  
<https://indico.fnal.gov/event/13795/>,  
<https://indico.him.uni-mainz.de/event/11/>,  
<http://www.int.washington.edu/PROGRAMS/19-74W/>.
- [10] D. Hanneke, S. Fogwell and G. Gabrielse, *Phys. Rev. Lett.* **100** (2008) 120801.
- [11] T. Aoyama, T. Kinoshita and M. Nio, *Phys. Rev. D* **97** (2018) 036001.
- [12] T. Aoyama, M. Hayakawa, T. Kinoshita and M. Nio, *Phys. Rev. Lett.* **109** (2012) 111807.
- [13] R. Bouchendira, P. Clade, S. Guellati-Khelifa, F. Nez and F. Biraben, *Phys. Rev. Lett.* **106** (2011) 080801.
- [14] R. H. Parker, C. Yu, W. Zhong, B. Estey and H. Müller, *Science* **360** (2018) 191.
- [15] S. Volkov, *Phys. Rev. D* **100** (2019) 096004.
- [16] A. Crivellin, M. Hoferichter and P. Schmidt-Wellenburg, *Phys. Rev. D* **98** (2018) 113002.
- [17] D. Nomura and T. Teubner, *Nucl. Phys. B* **867** (2013) 236.
- [18] J. Abdallah *et al.* [DELPHI Collaboration], *Eur. Phys. J. C* **35** (2004) 159.

- [19] S. Eidelman and M. Passera, *Mod. Phys. Lett. A* **22** (2007) 159.
- [20] S. J. Brodsky and E. de Rafael, *Phys. Rev.* **168** (1968) 1620.
- [21] B. E. Lautrup and E. de Rafael, *Phys. Rev.* **174** (1968) 1835.
- [22] K. Hagiwara, A. D. Martin, D. Nomura and T. Teubner, *Phys. Rev. D* **69** (2004) 093003.
- [23] B. Krause, *Phys. Lett. B* **390** (1997) 392.
- [24] A. Kurz, T. Liu, P. Marquard and M. Steinhauser, *Phys. Lett. B* **734** (2014) 144.
- [25] T. Xiao, S. Dobbs, A. Tomaradze, K. K. Seth and G. Bonvicini, *Phys. Rev. D* **97** (2018) 032012.
- [26] F. Jegerlehner (2003),  
<https://www-com.physik.hu-berlin.de/~fjeger/alphaQEDn.uu>.
- [27] A. Keshavarzi, D. Nomura and T. Teubner, in preparation.
- [28] F. Ambrosino *et al.* [KLOE Collaboration], *Phys. Lett. B* **670** (2009) 285.
- [29] F. Ambrosino *et al.* [KLOE Collaboration], *Phys. Lett. B* **700** (2011) 102.
- [30] D. Babusci *et al.* [KLOE Collaboration], *Phys. Lett. B* **720** (2013) 336.
- [31] A. Anastasi *et al.* [KLOE-2 Collaboration], *JHEP* **1803** (2018) 173.
- [32] B. Aubert *et al.* [BaBar Collaboration], *Phys. Rev. Lett.* **103** (2009) 231801.
- [33] G. Colangelo, M. Hoferichter and P. Stoffer, *JHEP* **1902** (2019) 006.
- [34] B. Ananthanarayan, I. Caprini and D. Das, *Phys. Rev. D* **98** (2018) 114015.
- [35] B. Ananthanarayan, I. Caprini, D. Das and I. Sentitemsu Imsong, *Phys. Rev. D* **89** (2014) 036007.
- [36] B. Ananthanarayan, I. Caprini, D. Das and I. Sentitemsu Imsong, *Phys. Rev. D* **93** (2016) 116007.
- [37] M. Davier, A. Hoecker, B. Malaescu and Z. Zhang, arXiv:1908.00921 [hep-ph].
- [38] M. Hoferichter, B. L. Hoid and B. Kubis, *JHEP* **1908** (2019) 137.
- [39] K. Hagiwara, A. D. Martin, D. Nomura and T. Teubner, *Phys. Lett. B* **649** (2007) 173.
- [40] K. Hagiwara, R. Liao, A. D. Martin, D. Nomura and T. Teubner, *J. Phys. G* **38** (2011) 085003.
- [41] M. N. Achasov *et al.*, *Phys. Rev. D* **98** (2018) 112001.
- [42] J. P. Lees *et al.* [BaBar Collaboration], *Phys. Rev. D* **98** (2018) 112015.
- [43] S. S. Gribov *et al.*, arXiv:1907.08002 [hep-ex].
- [44] M. N. Achasov *et al.*, *Phys. Rev. D* **99** (2019) 112004.

- [45] V. L. Ivanov *et al.*, Phys. Lett. B **798** (2019) 134946.
- [46] R. R. Akhmetshin *et al.* [CMD-3 Collaboration], Phys. Lett. B **792** (2019) 419.
- [47] F. Jegerlehner, arXiv:1711.06089 [hep-ph].
- [48] M. Davier, S. Eidelman, A. Höcker and Z. Zhang, Eur. Phys. J. C **31** (2003) 503.
- [49] M. Davier, Nucl. Phys. Proc. Suppl. **169** (2007) 288.
- [50] F. Jegerlehner, Nucl. Phys. Proc. Suppl. **162** (2006) 22.
- [51] M. Davier, A. Hoecker, B. Malaescu and Z. Zhang, Eur. Phys. J. C **71** (2011) 1515 [Erratum: Eur. Phys. J. C **72** (2012) 1874].
- [52] F. Jegerlehner and R. Szafron, Eur. Phys. J. C **71** (2011) 1632.
- [53] F. Jegerlehner, EPJ Web Conf. **166** (2018) 00022.
- [54] M. Davier, A. Hoecker, B. Malaescu and Z. Zhang, Eur. Phys. J. C **77** (2017) 827.
- [55] T. Aoyama, M. Hayakawa, T. Kinoshita and M. Nio, Phys. Rev. Lett. **109** (2012) 111808.
- [56] T. Ishikawa, N. Nakazawa and Y. Yasui, Phys. Rev. D **99** (2019) 073004.
- [57] C. Gnendiger, D. Stöckinger and H. Stöckinger-Kim, Phys. Rev. D **88** (2013) 053005.
- [58] J. Prades, E. de Rafael and A. Vainshtein, Adv. Ser. Direct. High Energy Phys. **20** (2009) 303.
- [59] F. Jegerlehner, EPJ Web Conf. **118** (2016) 01016.
- [60] V. Pauk and M. Vanderhaeghen, Eur. Phys. J. C **74** (2014) 3008.
- [61] A. Nyffeler, Phys. Rev. D **94** (2016) 053006.
- [62] M. Hoferichter, B. L. Hoid, B. Kubis, S. Leupold and S. P. Schneider, Phys. Rev. Lett. **121** (2018) 112002.
- [63] P. Masjuan and P. Sanchez-Puertas, Phys. Rev. D **95** (2017) 054026.
- [64] M. Hoferichter, B. L. Hoid, B. Kubis, S. Leupold and S. P. Schneider, JHEP **1810** (2018) 141.
- [65] G. Colangelo, M. Hoferichter, M. Procura and P. Stoffer, JHEP **1704** (2017) 161.
- [66] G. Colangelo, M. Hoferichter, M. Procura and P. Stoffer, Phys. Rev. Lett. **118** (2017) 232001.
- [67] G. Colangelo, F. Hagelstein, M. Hoferichter, L. Laub and P. Stoffer, arXiv:1910.13432 [hep-ph].
- [68] G. Colangelo, F. Hagelstein, M. Hoferichter, L. Laub and P. Stoffer, arXiv:1910.11881 [hep-ph].



- [69] M. Hoferichter at the INT Workshop INT-19-74W, University of Washington, WA (US), see <https://indico.fnal.gov/event/21626/session/9/contribution/49/material/slides/0.pdf>.
- [70] G. Colangelo, M. Hoferichter, A. Nyffeler, M. Passera and P. Stoffer, Phys. Lett. B **735** (2014) 90.
- [71] M. Steinhauser, Phys. Lett. B **429** (1998) 158.
- [72] C. Sturm, Nucl. Phys. B **874** (2013) 698.
- [73] K. G. Chetyrkin, J. H. Kühn and M. Steinhauser, Phys. Lett. B **371** (1996) 93; Nucl. Phys. B **482** (1996) 213; Nucl. Phys. B **505** (1997) 40.
- [74] J. H. Kühn and M. Steinhauser, Phys. Lett. B **437** (1998) 425.
- [75] F. G. Mariam *et al.*, Phys. Rev. Lett. **49** (1982) 993.
- [76] W. Liu *et al.*, Phys. Rev. Lett. **82** (1999) 711.
- [77] P. Strasser *et al.*, Hyperfine Interact. **237** (2016) 124.
- [78] P. J. Mohr, D. B. Newell and B. N. Taylor, Rev. Mod. Phys. **88** (2016) 035009.
- [79] M. I. Eides, Phys. Lett. B **795** (2019) 113.
- [80] S. G. Karshenboim, V. A. Shelyuto and A. I. Vainshtein, Phys. Rev. D **78** (2008) 065036.